3D Mouse Brain Reconstruction from Histology Using a Coarse-to-Fine Approach

Paul A. Yushkevich[1], Brian B. Avants[1], Lydia Ng[2], Michael Hawrylycz[2], Pablo D. Burstein[1], Hui Zhang[1], and James C. Gee[1]

[1] Penn Image Computing and Science Laboratory, Department of Radiology, University of Pennsylvania, Philadelphia PA, USA
[2] Allen Institute for Brain Science, Seattle WA, USA

Abstract. The Allen Brain Atlas project aims to bridge the divide between genomics and neuroanatomy by mapping the expression of the entire C57BL/6J mouse genome onto a high-resolution 3D anatomical reference atlas of the mouse brain. We present the image registration approach used to generate this anatomical reference from histological sections. Due to the large number of sections (525) and the presence of debris and distortions, a straightforward alignment of each slice to its neighbors fails to accurately recover the 3D shape of the brain. On the other hand, multimodality registration of histology slices to an MRI reference compromises correspondences between neighboring slices. Our approach combines the high-frequency component of slice-to-slice histology registration with the low-frequency component of the histology-to-MRI registration to produce a coarse-to-fine reconstruction that is accurate both in its global shape and in the alignment of local features.

1 Introduction

The problem of reconstructing a 3D volume from histological sections arises frequently in animal model research. In real experimental data, the reconstruction problem is made difficult by high incidence of artifacts such as tearing of tissue and debris. We present a new coarse-to-fine reconstruction algorithm that combines a graph-theoretic slice-to-slice reconstruction with a global histology-to-MRI reconstruction to achieve high accuracy both in the alignment of features between slices and in the 3D shape of the reconstructed brain. Our algorithm was used to generate the anatomical reference atlas of the mouse brain for the Allen Brain Atlas (ABA) project at the Allen Institute for Brain Science (AIBS).

The goal of the ABA project is to generate a freely accessible database of the expression of some 24,000 genes that compose the mouse genome. High resolution *in situ* hybridization in coronal and sagittal slices is used to map gene expression onto the reference atlas, allowing researchers to make complex queries relating gene expression and neuroanatomy [1]. Already, over 50% of the genome has been mapped and is available to researchers at `www.brain-map.org`.

J.P.W. Pluim, B. Likar, and F.A. Gerritsen (Eds.): WBIR 2006, LNCS 4057, pp. 230–237, 2006.

2 Prior Work

Often, the problem of volumetric reconstruction of the mouse brain is reduced to finding the appropriate 2D registration algorithm for aligning consecutive slices, and the 3D volume is constructed by concatenating the transformations resulting from pairwise registrations (e.g., [2]). As argued in Sec. 3.2, good interslice alignment does not guarantee accurate reconstruction of the 3D brain shape. In [3, 4], such reconstruction is followed by non-rigid 3D registration to MR microscopy data. In [5], the reconstruction problem is formulated as a simultaneous system of 2D elastic registrations, for which an efficient solver is available. The input to this system is a rigid reconstruction that uses the principal axis transformation, which is driven by the shape of slice outlines. The rigid reconstruction method presented in this paper is intensity-driven and should provide a better initialization for elastic registration. In the Harvard High Resolution Brain Atlas [6], 3D reconstruction is aided by landmarks that are identified manually. Similarly, [7] uses surface registration and hand-drawn contours to warp MRI data to histology. In contrast, our algorithm is automatic, allowing high throughput.

3 Materials and Methods

3.1 Histology and Reference MRI Data

The brain from a 56 day old sacrificed C57BL/6J strain mouse was surgically removed, chemically frozen and sectioned in the coronal plane into 525 0.25 μm thick slices using a microtome. Sections were fixed, treated with Nissl counterstain that stains nucleic acids in neuronal somata and dendrites, and imaged, producing high-resolution color images with pixel size 0.95 μm^2. While histological images capture incredible anatomical detail (Fig. 1d), they also tend to suffer from artifacts, such as stretching, tearing and displacement of tissue that occurs during microtomy, as well as debris that appear during slice preparation and staining. These artifacts are illustrated in Fig. 1a,b.

In addition to the histological data, we use a 3D reference volume that was constructed by averaging a set of 30 *in vivo* MRI scans from 10 mice of the same strain as the specimen used to generate histology data. The reference volume has voxel size 12.9 μm^3 and is shown in Fig. 3.

3.2 Coarse-to-Fine Reconstruction Overview

Due to the large number of slices and high incidence of artifacts, the straightforward approach of aligning and warping each slice to its neighbors and concatenating the resulting transformations does not yield acceptable results. In particular, the accumulation of errors can result in the *z-shift effect*, where, though each slice is registered well to its neighbors, the overall 3D shape of the reconstruction is distorted, such that the imaginary grid lines parallel to the z-axis in the true anatomy become curves in the reconstruction. Another problem is the propagation of errors due to the presence of highly distorted sections

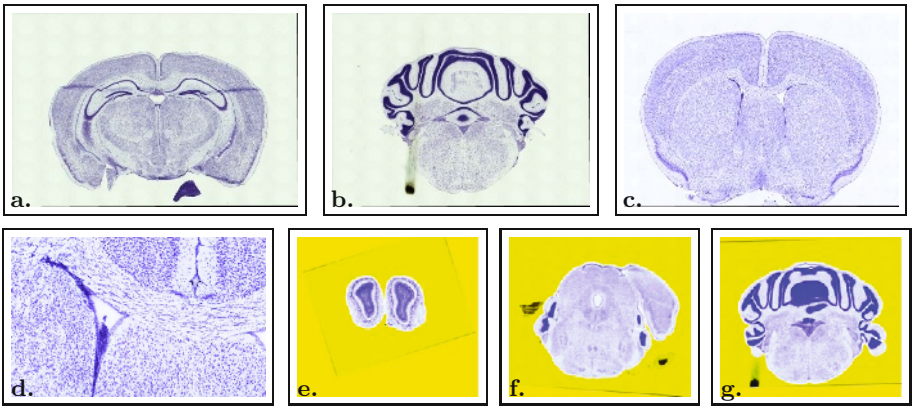

Fig. 1. a-d: Examples of Nissl-stained histological sections used in the reconstruction (**a:** a slice with tissue distortion; **b:** a slice with debris; **c:** an artifact-free slice; **d:** a subregion of slice **c** at full resolution). **e-f:** Examples of masks computed automatically for each slice. The region falling outside the mask is shaded yellow.

that are unlikely to register well to their neighbors and can cause gross discontinuities in the reconstructed anatomy. To address these issues, we developed a multi-stage method that combines segmentation, coarse-to-fine rigid reconstruction and deformable reconstruction to generate an atlas that is accurate both in terms of local anatomical continuity and global 3D brain shape.

We begin by giving an outline of our approach, with each step detailed in the subsequent sections. In the first stage, we use active contour segmentation to compute binary masks of the brain in each slice, so as to keep debris and dislodged tissue from contributing to the reconstruction. Next, we perform pairwise rigid registrations between neighboring slices to generate a locally accurate, fine-scale estimate of the reconstruction. By computing transforms not only between consecutive slices but between slices within a certain z-distance from each other, we reduce the z-shift and avoid negative effects of highly distorted slices. This initial 3D reconstruction is then registered to the reference MRI, producing a globally accurate, coarse-scale estimate of the reconstruction. The high-frequency component of the fine-scale estimate is then combined with the low-frequency component of the coarse-scale estimate to produce the final coarse-to-fine rigid reconstruction. This rigid reconstruction is then used to initialize a deformable registration, which produces a high quality 3D atlas.

3.3 Automatic Mask Computation

The background in histological slices can be highly inhomogeneous, containing debris, stains, and the edges of the glass plate. To keep these features from influencing slice alignment, we separate the brain from the background in each slice automatically, using a combination of active contour level set segmentation with

region competition [8] and mathematical morphology. The image force governing contour evolution is based on an estimate of object and background probabilities, which are estimated using thresholds. Active contour segmentation separates the brain from the more homogeneous background regions and island-like debris but it does not separate it from artifacts that are adjacent to it, such as the smear in Fig. 1c. We use erosion followed by dilation and taking the largest connected component to mask out such artifacts. Parameters of this masking approach may vary from slice to slice; however, in practice, a common set of parameters 'works' for over 90% of the slices; for the remaining slices, the researcher adjusts the parameters after examining the segmentation results. It may be possible to fully automate parameter selection in the future by using histogram analysis to set thresholds and by requiring masks computed on consecutive slices to have similar shape. Examples of masks are shown in Fig. 1e-g.

3.4 Fine-Scale Alignment

Our fine-scale alignment algorithm aims to minimize z-shift and the negative effects of badly distorted slices. This is accomplished by

1. Registering each histology slice not only to its nearest neighbors but also to neighbors located up to 5 slices away. The Insight Toolkit rigid registration pipeline [9] with the Mattes et al. mutual information metric [10] is used.
2. Constructing a weighted graph where the vertices represent the slices, the edges represent registrations between neighboring slices and the edge weights reflect the misregistration error, as detailed below.
3. Designating one slice as the reference and finding the shortest path from every vertex in the graph to the reference. These paths skip over those slices which register poorly to their neighbors, as Fig. 2 illustrates. For each slice, the chain of rigid transformations corresponding to the shortest path is concatenated, providing a rigid transformation from the slice to the reference.

The weight of the graph edge connecting vertices i and j is given by

$$W_{ij} = (1 + M_{ij})|i - j|(1 + \epsilon)^{|i-j|} \ , \tag{1}$$

where M_{ij} is the value of the mutual information metric mapped to the range $[0, 1]$ (smaller values correspond to better registration), and ϵ is a positive constant that modulates between too little slice skipping, which results in propagation of registration error due to distorted slices, and too much slice skipping, which can disturb fine-scale alignment between neighbor slices. When M_{ij} for all slice pairs are equal, no slices are skipped.

3.5 Coarse-Scale Alignment

To recover the gross shape of the mouse brain, we compute rigid registrations between histology slices and corresponding cross-sections of the reference MRI atlas. To compute the correspondences, we first use rigid 3D registration to

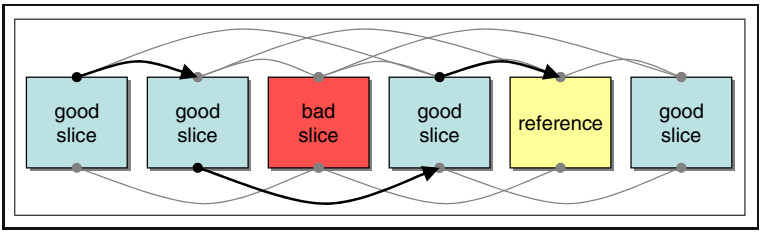

Fig. 2. An illustration of the graph-based reconstruction approach where each slice is registered to several neighbors and 'bad' slices (those that register poorly to neighbors) are skipped when aligning 'good' slices to the reference. Gray arcs indicate edges in the graph, i.e., transforms computed using rigid registration, and black arrows show the shortest path from the leftmost slice to the reference.

align the MRI volume to the histology volume reconstructed by the fine-scale algorithm; we then resample the MRI in the space of the histology volume, and extract 525 slices in the z-dimension. Both the 3D MRI-to-histology registration and the subsequent 2D histology-to-MRI registrations use the Mattes mutual information metric.

3.6 Coarse-Fine Recombination

The coarse and fine approaches described above produce 3D volumes that each have their own inadequacies. Fine-scale reconstruction aligns features well between neighboring slices, but does not eliminate z-shift. The coarse reconstruction attempts to recover the true shape of the brain, but it does so at the cost of local accuracy, as the registrations taking two neighboring histology slices into corresponding MRI slices are likely to disturb the alignment between the histology slices. In order to generate a single volume that fuses the attractive features of both reconstructions, we combine the high-frequency component of the fine-scale reconstruction with the low-frequency component of the coarse-scale reconstruction. This is achieved simply by smoothing across the z dimension the parameters of the transforms that map histology slices into corresponding MRI slices. Gaussian smoothing with $\sigma = 100\mu$m is applied to each component of the rigid transforms between histology and MRI. This makes the mapping from the fine-scale histology reconstruction into the MRI volume smooth across the z axis, maintaining the local correspondences established during slice-to-slice histology registration, while shifting the overall shape of the reconstructed volume to match that of the MRI brain. The choice of σ was made empirically by estimating that the misregistration error of histology-to-MRI registration is approximately equal to four times the error in histology-to-histology registration.

3.7 Diffeomorphic Reconstruction

The deformable component of our reconstruction method will be presented elsewhere and is not the focus of the present paper. We summarize it here for the

sake of completeness. The reconstruction borrows the ideas from mesh fairing algorithms, where meshes are smoothed by moving each vertex to the average of its neighbors over a number of iterations. In our iterative method, each slice is deformed towards the average of its neighbors using a diffeomorphic inverse consistent algorithm [11]. This iterative deformation essentially smooths the shape of anatomical structures across the z dimension. Akin to variable conductance diffusion, badly distorted slices, which are identified during rigid reconstruction, are assigned low weights in the iterative shape averaging process, preventing the distortions from propagating into neighboring slices, while allowing the good slices to influence the deformation of their badly distorted neighbors.

4 Results

Sagittal and horizontal cross-sections of the fine-scale, coarse-scale and coarse-to-fine rigid reconstructions are shown in Fig. 3. The thick blue outline indicates

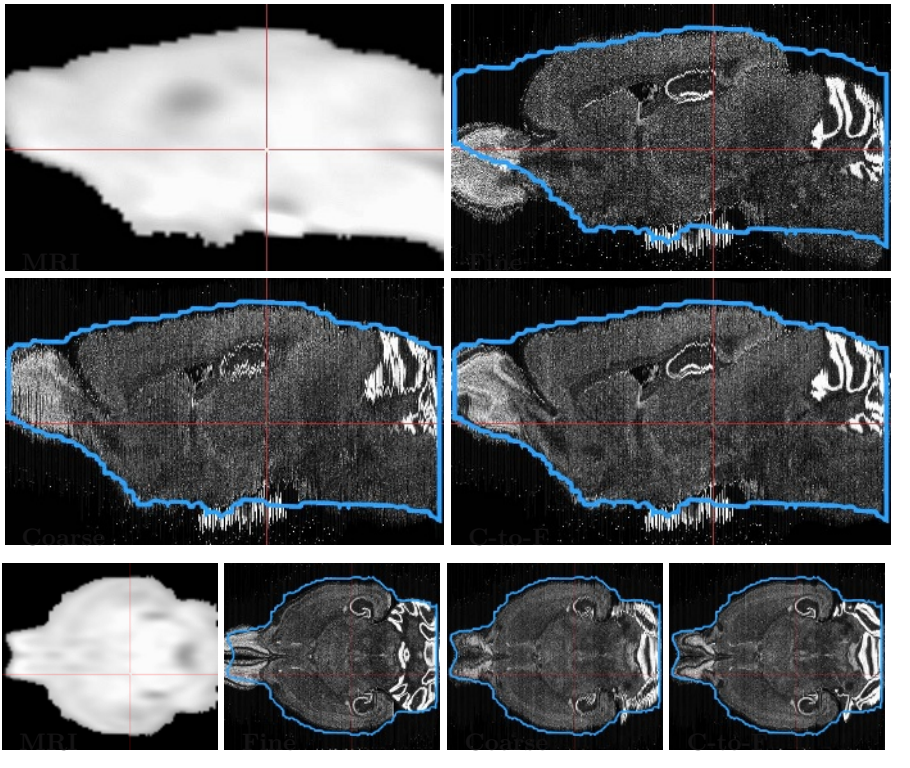

Fig. 3. MRI-based reference image and results of rigid histology reconstruction, including fine-scale reconstruction (slice-to-slice histology), fine-scale reconstruction (histology-to-MRI) and combined coarse-to-fine reconstruction. The outline of the brain surface in the MRI reference is overlaid as a blue curve on the reconstruction results.

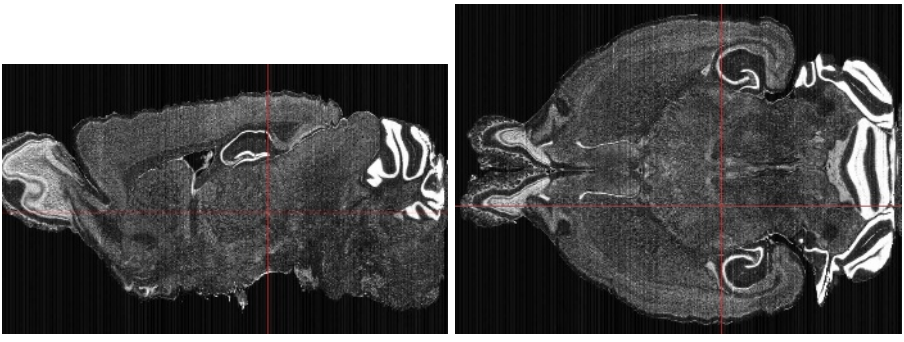

Fig. 4. Deformable reconstruction result

the boundary of the brain in the MRI reference. The z-shift occurring in fine-scale reconstruction is clearly evident, particularly in the sagittal cross-section. Poor local alignment of the coarse-scale rigid reconstruction is evident when comparing the cerebellum and other high-contrast structures between fine-scale and coarse-scale reconstructions. Visual inspection of the coarse-to-fine rigid reconstruction shows that it is superior to both fine-scale and coarse-scale reconstructions. The results of the deformable reconstruction are shown in Fig 4. Given the excellent initialization provided by the rigid method, the deformable method produces a reconstruction that is accurate in terms of both the overall 3D shape and the continuity of anatomical features across the z dimension.

5 Discussion and Conclusions

A drawback of our method is the number of parameters that are chosen empirically. These include parameters for mask computation, the factors in computing the weights of the graph in fine-scale reconstruction and the width of the Gaussian filter used in the coarse-fine combination. It is difficult to set optimal values for these parameters because the ground truth against which the reconstruction result could be compared is not available. To a great extent, we rely on visual inspection to assess reconstruction quality but our future work will focus on generating quantitative assessments. One potential approach is to measure how well our reconstruction from coronal slices can match sagittal sections obtained from specimens from the same strain. This 2D/3D registration metric is especially useful because the ABA reference atlas itself is subsequently used as a reference to which slices from sagittal *in situ* hybridization are registered.

In conclusion, we have presented the details of a coarse-to-fine rigid 3D reconstruction technique for histological data. The approach combines the local accuracy of intensity-based registration between neighboring slices with the global accuracy of registration to a reference MRI dataset. Our results indicate that the combined coarse-to-fine approach is superior to either of its coarse and fine components taken on their own. Followed up with deformable diffeomorphic

reconstruction, our approach generates a high quality anatomical murine brain atlas that has been adopted by the Allen Institute for Brain Science as the reference for mapping gene expression.

Acknowledgement

This work was made possible through funding support from the Allen Institute for Brain Science.

References

1. Lydia Ng, Michael Hawrylycz, and David Haynor. Automated high-throughput registration for localizing 3D mouse brain gene expression using ITK. *Insight Jounral*, 1, 2005. Special Issue on ISC/NA-MIC/MICCAI Workshop on Open-Source Software.
2. S. Ourselin, A. Roche, G. Subsol, X. Pennec, and N. Ayache. Reconstructing a 3D structure from serial histological sections. *Image and Vision Computing*, 19(1):25–31, Jan 2001.
3. Allan MacKenzie-Graham, Erh-Fang Lee, Ivo D Dinov, Mihail Bota, David W Shattuck, Seth Ruffins, Heng Yuan, Fotios Konstantinidis, Alain Pitiot, Yi Ding, Guogang Hu, Russell E Jacobs, and Arthur W Toga. A multimodal, multidimensional atlas of the C57BL/6J mouse brain. *J Anat*, 204(2):93–102, Feb 2004.
4. S. Ourselin, E. Bardinet, D. Dormont, G. Malandain, A. Roche, N. Ayache, D. Tande, K. Parain, and J. Yelnik. Fusion of histological sections and mr images: Towards the construction of an atlas of the human basal ganglia. In *Medical Image Computing and Computer-Assisted Intervention, MICCAI*, pages 743–751, London, UK, 2001. Springer-Verlag.
5. Stefan Wirtz, Nils Papenberg, Bernd Fischer, and Oliver Schmitt. Robust and staining-invariant elastic registration of a series of images from histologic slices. In J. Michael Fitzpatrick and Joseph M. Reinhardt, editors, *Medical Imaging 2005: Image Processing*, volume 5747, pages 1256–1262. SPIE, 2005.
6. R.L. Sidman, B. Kosaras, B. Misra, and S. Senft. High resolution mouse brain atlas, 2005. http://www.hms.harvard.edu/research/brain.
7. M. A. Jacobs, J. P. Windham, H. Soltanian-Zadeh, D. J. Peck, and R. A. Knight. Registration and warping of magnetic resonance images to histological sections. *Med Phys*, 26(8):1568–78, Aug 1999.
8. Song Chun Zhu and Alan Yuille. Region competition: Unifying snakes, region growing, and bayes/mdl for multiband image segmentation. *IEEE Trans. Pattern Anal. Mach. Intell.*, 18(9):884–900, 1996.
9. L. Ibanez, W. Schroeder, L. Ng, and J. Cates. *The ITK Software Guide*. Kitware, Inc., 2003.
10. David Mattes, David R. Haynor, Hubert Vesselle, Thomas K. Lewellyn, and William Eubank. Nonrigid multimodality image registration. In Milan Sonka and Kenneth M. Hanson, editors, *Medical Imaging 2001: Image Processing*, volume 4322, pages 1609–1620. SPIE, 2001.
11. B. Avants, P.T. Schoenemann, and J.C. Gee. Lagrangian frame diffeomorphic image registration: Morphometric comparison of human and chimpanzee cortex. *Medical Image Analysis*, 2005. In Press.